Side-band Algorithm for Automatic Wind Turbine Gearbox Fault Detection and Diagnosis

D. Zappalá[1*], P. J. Tavner[1], C. J. Crabtree[1], S. Sheng[2]

[1]*School of Engineering and Computing Sciences, Durham University, Durham, DH1 3LE, UK*
[2]*National Renewable Energy Laboratory (NREL), Golden, Colorado, 80401, USA*
[*]*Corresponding author: donatella.zappala@durham.ac.uk*

Abstract

Improving the availability of wind turbines (WT) is critical to minimising the cost of wind energy, especially offshore. The development of reliable and cost-effective gearbox condition monitoring systems (CMS) is of concern to the wind industry, because gearbox downtime has a significant impact on WT availabilities. Timely detection and diagnosis of developing gear defects is essential to minimise unplanned downtime. One of the main limitations of most current CMSs is the time-consuming and costly manual handling of large amounts of monitoring data, therefore automated algorithms would be welcome. This paper presents a fault detection algorithm for incorporation into a commercial CMS for automatic gear fault detection and diagnosis. Based on experimental evidence from the Durham condition monitoring test rig, a gear condition indicator was proposed to evaluate the gear damage during non-stationary load and speed operating conditions. The performance of the proposed technique was then successfully tested on signals from a full-size WT gearbox that had sustained gear damage, and had been studied in a National Renewable Energy Laboratory's (NREL) programme. Results show that the proposed technique proves efficient and reliable for detecting gear damage. Once implemented into WT CMSs, this algorithm can automate data interpretation, reducing the quantity of information that WT operators must handle.

1. Introduction

The European Wind Energy Association estimates that by 2020 230GW of wind capacity will be installed in Europe and 735GW will be installed by 2050 [1]. These targets cannot be met without large-scale offshore wind development in increasingly remote and hostile locations. In these environments installation is more difficult and expensive and access to the wind farms for maintenance is also limited. Due to the reduced site accessibility and the high cost of specialist personnel and equipment involved offshore operation and maintenance (O&M) costs can be quantified as three to five times higher than those on land [2]. O&M costs are estimated to account for up to 30% of the energy generation costs, with a considerable part, around 70%, caused by unexpected failures [3]. These high figures make the energy produced less competitive compared to conventional sources and emphasize the need for optimizing the O&M strategy for offshore wind farms to reduce turbine downtime and increase availability. Achieving high WT availability is paramount to providing affordable and cost-effective wind energy. Offshore, the reactive maintenance strategies often employed onshore are largely impractical due to difficulties in wind farm access as a result of harsher environmental conditions. The adoption of Condition-Based Maintenance (CBM) can contribute significantly to minimize offshore O&M costs by lowering the number of inspection visits and corrective maintenance actions [4]. This maintenance approach involves repair or replacement of parts based on their actual condition and the individual operating history of the particular machine, rather than on a schedule based on predicted operating conditions of the average machine [5]. The development of reliable and cost-effective condition monitoring techniques, with automatic damage detection and diagnosis of WT components, plays a pivotal role in establishing technically and economically viable CBM strategies, especially for unattended WTs located in remote and difficult-to-access locations. Autonomous on-line CMSs allow early warning of mechanical and electrical defects to prevent major component failures. Faults can be detected while the defective component is still operational and thus necessary repair actions can be planned in time.

2. Wind Turbine Gearbox Condition Monitoring

Among the various WT components, the gearbox has been shown to cause the longest downtime [6] and is the most costly to maintain throughout a turbine's 20-year-plus design life [7]. Gearbox faults, with high replacement costs, complex repair procedures, and revenue loss caused by long downtime, are widely considered a leading issue for WT drive train condition monitoring (CM) [5, 8, 9]. Common WT gearbox failure modes are bearing faults and gear tooth damage [10]. The stochastically varying torque on the gearbox is considered to be a major root cause for bearing and gear wear, driving gearbox failure modes and affecting gearbox life. Typical gear faults include pitting, scuffing, chipping and more seriously, cracks [11]. A recent study [12] has shown that the gearbox alone could be responsible for up to one-third of all lost onshore WT availability. This problem is exacerbated offshore where harsh weather and sea conditions could prevent maintenance or component replacement for long periods of time. Few reliability data are still publicly available for offshore WTs. However, 3 years of available data from Egmond aan Zee wind farm in the Netherlands show how the gearbox downtime caused 55% of the total wind farm downtime [13].

The main WT Operator concerns about gearbox reliability, particularly offshore, are:

- High replacement costs following a failure;
- Complex repair procedures that incur high logistics costs and require favourable weather conditions [10];
- High revenue losses caused by long downtime between failures and repair completion.

Consequently, the gearbox has become an essential subject for current commercial WT CMS. Timely and reliable detection and diagnosis of developing gear defects within a gearbox is an essential part of minimizing unplanned downtime of WTs. WT CMS application was requested by insurance companies in Europe in the late 1990s, following a large number of claims triggered by catastrophic WT gearbox failures [14], although these root causes have largely been eliminated by changes in WT

design. Today, a number of commercial WT CMSs are available to the wind industry and they are largely based upon experience of monitoring conventional rotating machines. A cost-benefit analysis has shown that the lifetime savings derived from early warning and avoidance of impeding failures of the critical WT components would more than offset the lifetime cost of a CM system [11].

A survey carried out by the UK Supergen Wind Energy Technologies Consortium [15] shows that the most popular CM approach for the gearbox is vibration monitoring using traditional Fourier transform analysis of high frequency data to detect fault-specific frequencies. However, applying vibration-based CM to WTs presents a few unique challenges. WTs are variable load and speed systems operating under highly dynamic conditions, usually remote from technical support. This results in CM signals which are dependant not only on component integrity but also on the operating conditions. One limitation of the conventional Fast Fourier Transform (FFT) analysis is its inability to handle non-stationary waveform signals which may not yield accurate and clear gearbox features. In order to acquire directly comparable data and to allow spectra to be recorded in apparently stationary conditions, a number of commercial CMSs can be configured to collect the vibration spectra within limited, pre-defined speed and power ranges [15]. To overcome the problems of conventional FFT-based techniques and find improved solutions for WT CM, a number of advanced signal processing techniques, including wavelet transforms, time-frequency analysis and Artificial Intelligence (AI) techniques, have been also researched recently [8, 16-18]. However, most new techniques are unsuitable for on-line CM use, because they are computing intensive, and have not been demonstrated yet in operating WTs.

One major limitation of the current commercial available CMSs is that very few operators make use of the alarm and monitoring information available to manage their maintenance because of the volume and complexity of the data. In particular, the frequent false alarms and the costly specialist knowledge, required for manual interpretation of the complex vibration data, have discouraged WT operators from making wider use of CMS. This happens despite the fact that these systems are fitted to the majority of large WTs (>1.5 MW) in Europe [18]. Moreover, with the growth of the WT

population, especially offshore, the manual examination and comparison of the CM data will be impractical unless a simplified monitoring process is introduced.

Current efforts in the wind condition monitoring industry are aimed at automating data interpretation and improving the accuracy and reliability of diagnostic decisions, especially in the light of impending large-scale, offshore wind-farm generation. This study attempts to target this research area by experimentally defining an algorithm that could be incorporated into current CMS for automatic gear fault detection and diagnosis. This algorithm could reduce the quantity of information that the WT operators must handle, providing improved detection and timely decision-making capabilities.

The paper initially investigates the effect of gear tooth fault severity on the gearbox vibration signature using experimental results obtained from the 30 kW Wind Turbine Condition Monitoring Test Rig (WTCMTR) at Durham University. A frequency tracking algorithm that automatically detects and diagnoses gear tooth faults is proposed and discussed. The performance of the proposed technique is then tested using 750 kW gearbox data sets from the National Renewable Energy Laboratory's (NREL) Wind Turbine Gearbox Condition Monitoring Round Robin project [19]. These vibration signals were collected from a real WT gearbox that had sustained gear damage during its field test.

3. Experimental Methodology

3.1. Durham Wind Turbine Condition Monitoring Test Rig

Experimental research was performed on a 30 kW WTCMTR at Durham University, shown in Figure 1, which has been designed to act as a model for a WT drive train. The rig features a 54 kW DC motor driving a 3-phase, 4-pole, 30 kW wound rotor induction generator (WRIG) through a two-stage helical-gear parallel shaft gearbox. The first low-speed (LS) stage teeth 66/13 and second high-speed (HS) stage 57/58 provide an overall gear ratio of 5:1 (4.9894:1). A complete description of the test rig and instrumentation can be found in [20].

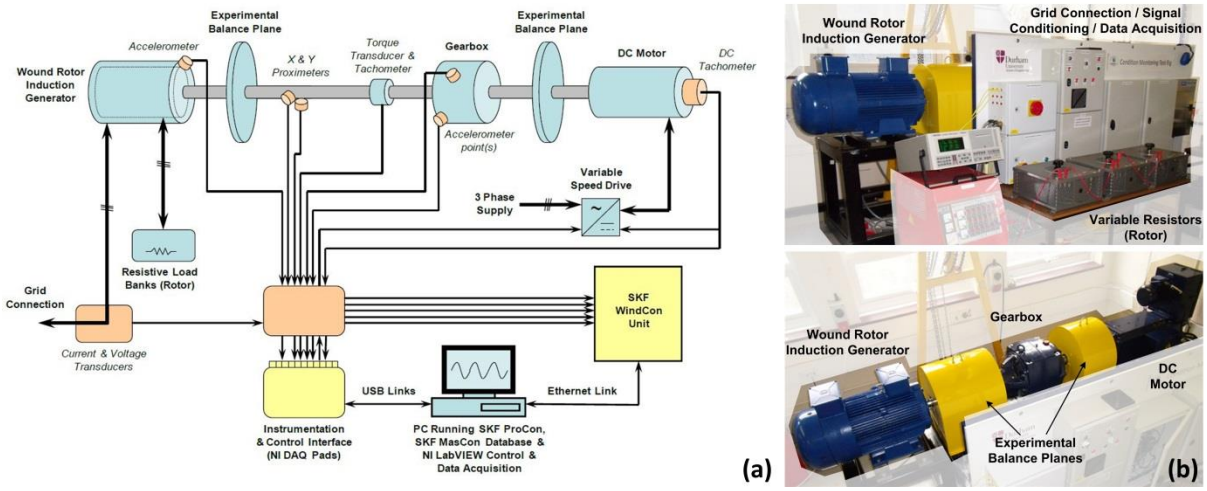

Figure 1: Durham WTCMTR: (a) Schematic diagram; (b) main components, instrumentation and control systems [20].

The WRIG has external variable resistors connected to the rotor circuit that allowed a super-synchronous generator speed variation of 100 rev/min, from 1500 to 1600 rev/min, with a corresponding maximum power output of 3.6 kW. The DC motor was driven at constant and wind-like variable speed conditions to cover the allowed speed range. Variable speed machine testing was performed using driving data derived from a 2 MW WT model [20]. Vibration data from a single-axis, vertically mounted accelerometer located on the gearbox high speed stage (HSS) were processed using an SKF WindCon unit 3.0, a commercial CMS producing FFT spectra, as currently used on full-size operational WTs. The sensor used was a piezoelectric accelerometer with integral electronics and a sensitivity of 500 mV/g.

3.2. Experimental Procedure and Data Observation

In a geared transmission system a main vibration source is the meshing action of the gears. The geometry of the gear profile has a crucial effect on the vibration behaviour. In practice, as the teeth deform under load, a meshing error is introduced even when the tooth profiles are perfect. In addition there are geometric deviations from the ideal profiles, due to gear manufacturing errors [16]. The most important components in gear vibration spectra are the tooth meshing frequencies and their harmonics, together with side-bands (SB) caused by modulation phenomena due to mean geometric errors on the tooth profiles, machining errors and wear. The gear meshing frequency is

defined as the product of the number of teeth on the gear and its turning speed. For gearboxes in good condition, the SB level generally remains constant with time. Therefore, the increment in the number and amplitude of such SBs may indicate a fault condition [17]. Local tooth damage produces short-duration impacts that add amplitude and frequency modulation effects to the meshing vibration, and in turn generate a higher level of SBs around the mesh harmonics. Moreover, the spacing of the SBs is related to their source and thus contains important diagnostic information [21]. In particular, the localised modulation effect takes place only during the engagement of the faulted teeth, but repeated once each revolution of the gear. As a consequence, the spectrum presents a large number of SBs of the tooth meshing frequency and its harmonics spaced by the faulted gear rotational frequency. Typically, the more damage that occurs, the more energy there is in the SBs [22]. In particular, previous literature on vibration analysis has shown that monitoring the second harmonic of gear mesh and its SBs allows early detection of gear wear [23].

Experiments were conducted to investigate the progression of a tooth defect on a high speed shaft (HSS) pinion, which was introduced into the WTCMTR at variable-speed and generator load. The behaviour of a healthy pinion and of four faults of increasing severity were investigated by introducing progressive damage to the leading contact edge of one tooth of the gearbox pinion. These are called seeded-fault tests. Figure 2(a) shows the healthy pinion, Figures 2(b), (c), and (d) show early stages of tooth wear, while Figure 2(e) depicts the entire tooth missing. Vibration data from the accelerometer were processed by WindCon assuming a fixed sampling frequency and producing FFT spectra with an overall frequency range of 5 kHz in the 1500-1600 rev/min HSS active range. The accelerometer measurement point in WindCon has been configured to provide vibration spectra which refer to a measurement time window of 1.28 sec. The produced spectra have 6400 resolution lines for a 5 kHz bandwidth with a resulting frequency resolution of 0.78125 Hz/Line. WindCon's built-in diagnostic tools have been used to assist with the analysis of the spectra by tracking the machine component-specific, speed-dependent fault frequencies, their harmonics and SBs.

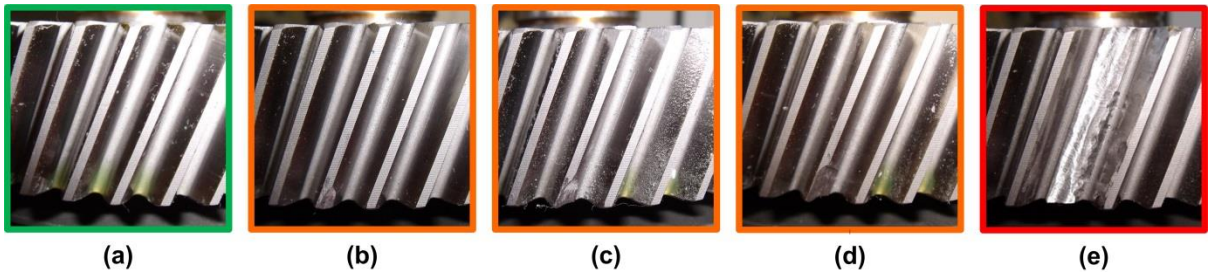

Figure 2: HSS pinion conditions investigated during the seeded-fault tests: (a) healthy; early stage of tooth wear: (b) 3-mm x 2-mm chip; (c) 5-mm x 5-mm chip; (d) 7-mm x 5-mm chip; (e) missing tooth.

Normalised order spectra (X) were used to facilitate the comparison of spectra and to identify the effect of a faulty tooth on the 30 kW gearbox vibration signature. A local gear defect, such as a cracked tooth, generates a disturbance each revolution. Basically a spectral order is introduced as a non-dimensional frequency parameter. If the frequency axis is normalised to the shaft rotation frequency any cyclic event synchronised with the shaft rotation will produce a spectral component at a fixed position even under variable speed conditions. The advantage of this approach is that it is easier to focus on a specific cyclic mechanism. During the tests performed on the Durham WTCMTR the HSS speed signal was recorded simultaneously with the vibration data by the WindCon software. The WindCon's frequency unit has a built-in tool allowing the operator to switch easily and automatically between Hz or Order frequency units. This is done by dividing the FFT frequency in Hz by the HSS rotational speed, f_{HSS}, at which the spectrum was collected. The FFT spectra produced were compared under similar machine operating conditions. Measured data showed that the presence of a HSS pinion faulty tooth results in clear and prominent f_{HSS} SB components of HS stage meshing frequency second harmonic, $2xf_{mesh,HS}$, in the vibration signal. For this reason, monitoring the second harmonic narrowband window has been assumed as the most reliable and consistent indicator of HSS pinion fault [24]. Figure 3 shows the zoom-in view of the measured HSS order vibration spectra around the $2xf_{mesh,HS}$ second harmonic, given by

$$2xf_{mesh,HS} = 116X \quad (1)$$

for healthy, early stages of tooth wear and missing tooth conditions at a typical operating speed of 1560 rev/min and 51% of maximum generator output.

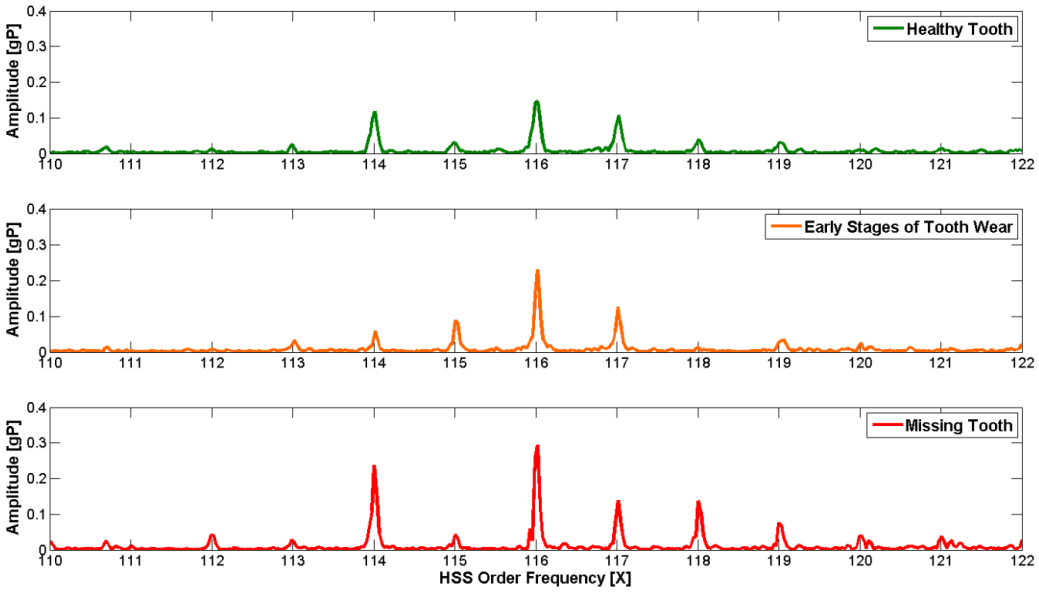

Figure 3: 30 kW gearbox FFT vibration spectra during the seeded-fault tests in the [110-120]X HSS Order frequency bandwidth.

The spectra show an increase in signal harmonic content as a result of abnormal gear-set behaviour due to the progressive damage introduced to the gearbox HSS pinion. The presence of the faulty pinion can be clearly seen in the $2xf_{mesh,HS}$ harmonic which is heavily modulated by the HSS speed, f_{HSS}, given by

$$f_{HSS} = 1X \tag{2}$$

Ten SBs of the $2xf_{mesh,HS}$ harmonic, SB_i, calculated as

$$SB_i = \left(2xf_{mesh,HS} \pm i\right)X \tag{3}$$

where $i = \pm 1, \pm 2, \pm 3, \pm 4, \pm 5$, are visible in the spectra. The severity level of the tooth damage affects the SB amplitudes. Furthermore, the gear mesh centre harmonic, surrounded by the SBs, denotes which gear mesh the damaged gear is passing through. These two pieces of information indicate that

the damaged component is passing through the HS stage gear mesh and is mounted on the HSS shaft.

3.3. Algorithm Definition

The seeded-fault tests conducted in this study show that the presence of meshing frequency harmonic SBs and their amplitudes could be valuable for detecting and diagnosing gear defects. However, the manual analysis of the spectra, needed to compare the changes in amplitudes for different conditions, requires significant time-consuming work due to the great number of frequency bands to be monitored. This calls for intelligent monitoring strategies that are able to detect faulty signal in an automatic way. The suggestion is to track the overall power of the spectra associated with the $2xf_{mesh,HS}$ SB frequency window. Based on the experimental evidence, a gear condition indicator, the SB Power Factor (SBPF) algorithm, has been proposed to evaluate the gear damage during the WT non-stationary load and speed operating conditions [24]. The SBPF algorithm sums the Power Spectrum amplitudes of the HS stage meshing frequency second harmonic and its first 5 SB peaks on each side. It has been calculated using

$$SBPF = PSA(2xf_{mesh,HS}) + \sum_{i=-5}^{+5} PSA(SB_i) \quad (4)$$

where $PSA(2xf_{mesh,HS})$ and $PSA(SB_i)$, with $i = \pm1,\pm2,\pm3,\pm4,\pm5$, are the power spectrum amplitudes of the $2xf_{mesh,HS}$ harmonic and of its first 5 SBs spaced at the HSS rotational speed, respectively, shown in Figure 4. The proposed algorithm facilitates the monitoring analysis, reducing each FFT spectrum to only one parameter for each data acquisition and avoiding time-consuming manual spectra comparison.

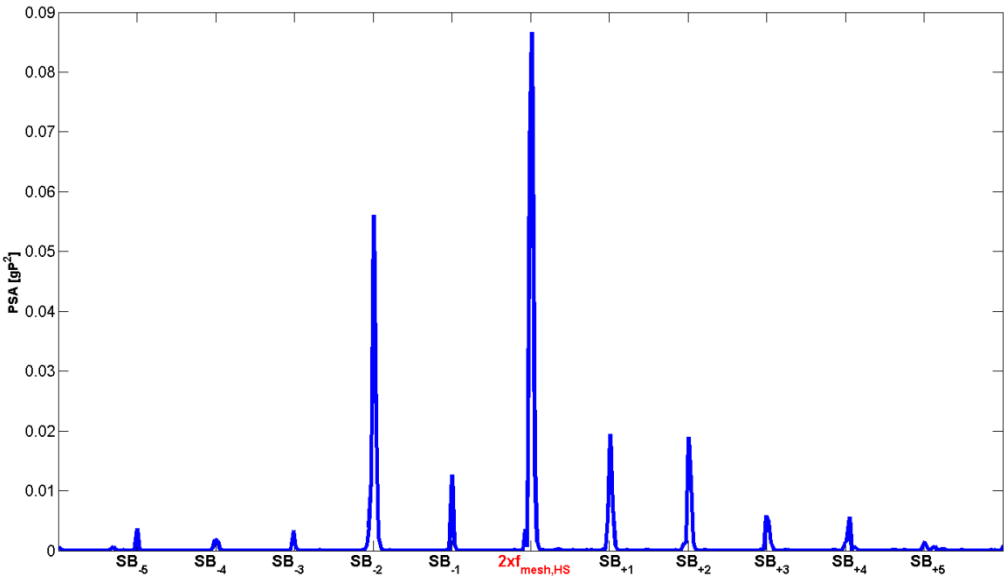

Figure 4: Typical FFT Power Spectrum around the $2xf_{mesh,HS}$ harmonic in the case of faulty HS Pinion.

3.4. Results

The influence of the fault severity and the variable load operating conditions on the SBPF values has been investigated by performing variable speed tests on the WTCMTR at a load up to 3.6 kW. The resulting SBPF values are shown in Figure 5 against the load, expressed as a percentage of the maximum generator output in this condition, for HSS pinion healthy conditions, for early stages of tooth wearing, and for a missing tooth. No frequency averaging has been performed on the data before the extraction of SBPF values.

The results show that the SBPF magnitude is proportional to the magnitude of the gear fault level. This is because as damage develops on a gear tooth passing through the gear mesh, the SBs increase in amplitude, resulting in larger SBPF values. The trend of the obtained SBPF values can be fitted by an exponential curve, relating vibration spectra power increase with machine load. In the full range of the load investigated, the SBPF values for the missing tooth case are higher than both the healthy and early tooth wear cases, indicating clear fault detection. The proposed algorithm works successfully even at the early stages of the tooth failure, showing a higher effectiveness at percentage loads above 20%.

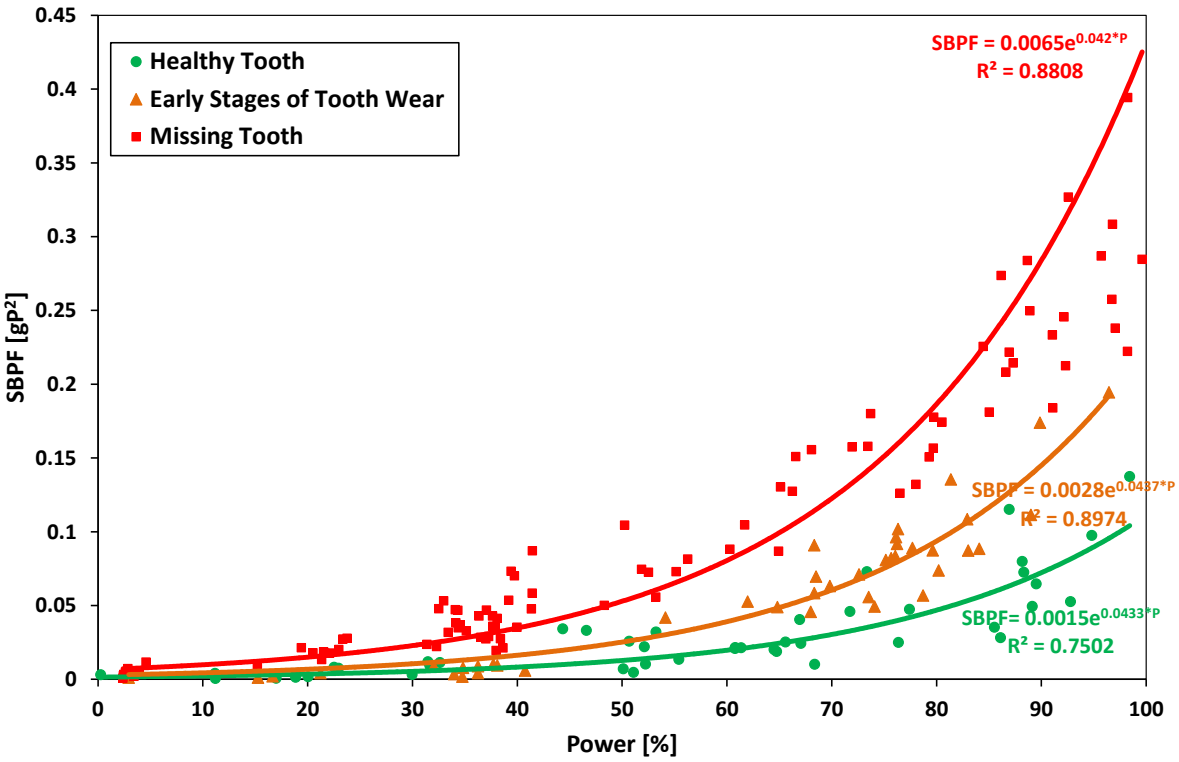

Figure 5: Influence of the fault severity and the variable load operating conditions on the SBPF values during the seeded-fault tests.

4. Algorithm Validation

4.1. NREL Wind Turbine Gearbox Condition Monitoring Round Robin Project

To validate the performance and reliability of the proposed SBPF algorithm on a full-size gearbox, the algorithm has been tested on data from the NREL Wind Turbine Gearbox Condition Monitoring Round Robin project [19]. Vibration data collected from two identical 750 kW WT gearboxes, tested on the NREL dynamometer test stand in Figure 6, were used in this study. A complete description of the NREL test-bed and instrumentation can be found in [25]. The gearboxes have an overall ratio of 1:81.491 and feature one low-speed (LS) planetary stage and two parallel stages, an intermediate-speed (IS) and high-speed (HS) stage, respectively. Table 1 provides details of the NREL gearbox nomenclature for the internal elements and the gear teeth number.

Figure 6: NREL dynamometer test stand with 750 kW gearbox installed.
Photo by Lee Jay Fingersh / *NREL 16913*.

Table 1: NREL 750 kW gearbox nomenclature and teeth number.

Gear Element	Location	Number of Teeth	Mate Teeth	Ratio
Ring Gear	LS Planetary Stage	99	39	
Planet Gear	LS Planetary Stage	39	99	
Sun Pinion	LS Planetary Stage	21	39	5.71
Intermediate Gear	IS Parallel stage	82	23	
Intermediate Pinion	IS Parallel stage	23	82	3.57
HSS Gear	HS Parallel stage	88	22	
HSS Pinion	HS Parallel stage	22	88	4.0
			Overall Ratio:	81.491

Baseline data were collected on the dynamometer test stand from a healthy test gearbox, which had no operational experience. Data then were collected from the dynamometer re-test of an identical gearbox after its internal components had sustained damage from its field test. This gearbox first finished a run-in in the NREL dynamometer and was then sent to a nearby wind farm for a field test. The test gearbox was installed on a three-blade, stall-regulated, upwind WT with a rated power of 750 kW and a rated wind speed of 16 m/s. In the field, two oil loss events occurred and led to some damage to gears and bearings inside the test gearbox. The gearbox was then removed from the field

and retested under controlled conditions in the NREL test stand. During the re-test, various condition monitoring data were collected, including measurements of vibration and oil debris. Once the dynamometer retest was completed, the gearbox was disassembled and a detailed failure analysis was conducted [26]. Severe scuffing of the HS shaft gear set was one of 12 instances of damage found during the failure analysis. Figure 7 shows the damaged HSS pinion.

Figure 7: Pinion damage on the 750 kW gearbox HSS. Photo from GEARTECH /*NREL 19743*.

4.2. Vibration Data Analysis

The task of this study was to validate the SBPF analysis of vibration data to detect and diagnose HSS pinion damage using data collected by two independent accelerometers, AN6 and AN7, mounted radially on the gearbox intermediate-speed shaft (ISS) and HSS, respectively. Both of these sensors were integrated-circuit piezoelectric-type accelerometers with a sensitivity of 100 mV/g.

The available data-set refers to an HSS speed of 1800 rev/min and to 50% of rated power, which is the highest test load applied to reduce the chances of a catastrophic gearbox failure. For each accelerometer, it contains:

- For the healthy gearbox: 1 single FFT spectrum collected by a commercial CMS at 5 kHz for a duration of 1.6 sec.
- For the faulty gearbox: 40 kHz raw vibration data collected continuously for 10 minutes.

The data-set presented some challenges for deriving an SB amplitude comparison system baseline. This was overcome by windowing data from the faulty gearbox through a 1.6 sec time window and then processing the data using the built-in FFT algorithm in MATLAB. For each accelerometer, the resulting 375 FFT spectra have then been consistently compared against the available healthy

spectrum, presenting the same frequency resolution. Figure 8 a) and b) show an example of the zoom-in view of the healthy and faulty HSS order vibration spectra around the HS stage meshing frequency second harmonic, $2xf_{mesh,HS}$, given by

$$2xf_{mesh,HS} = 44X \quad (5)$$

for the AN6 and AN7 accelerometer data, respectively.

In both cases, when comparing the degraded gearbox to the nominal baseline healthy gearbox, the increase in energy content of the $2xf_{mesh,HS}$ harmonic and its SBs can be clearly seen. In the faulty spectrum, the HS meshing frequency second harmonic is heavily modulated by the HSS rotational speed, $f_{HSS} = 1X$. The SB spacing indicates severe damage in the HSS pinion.

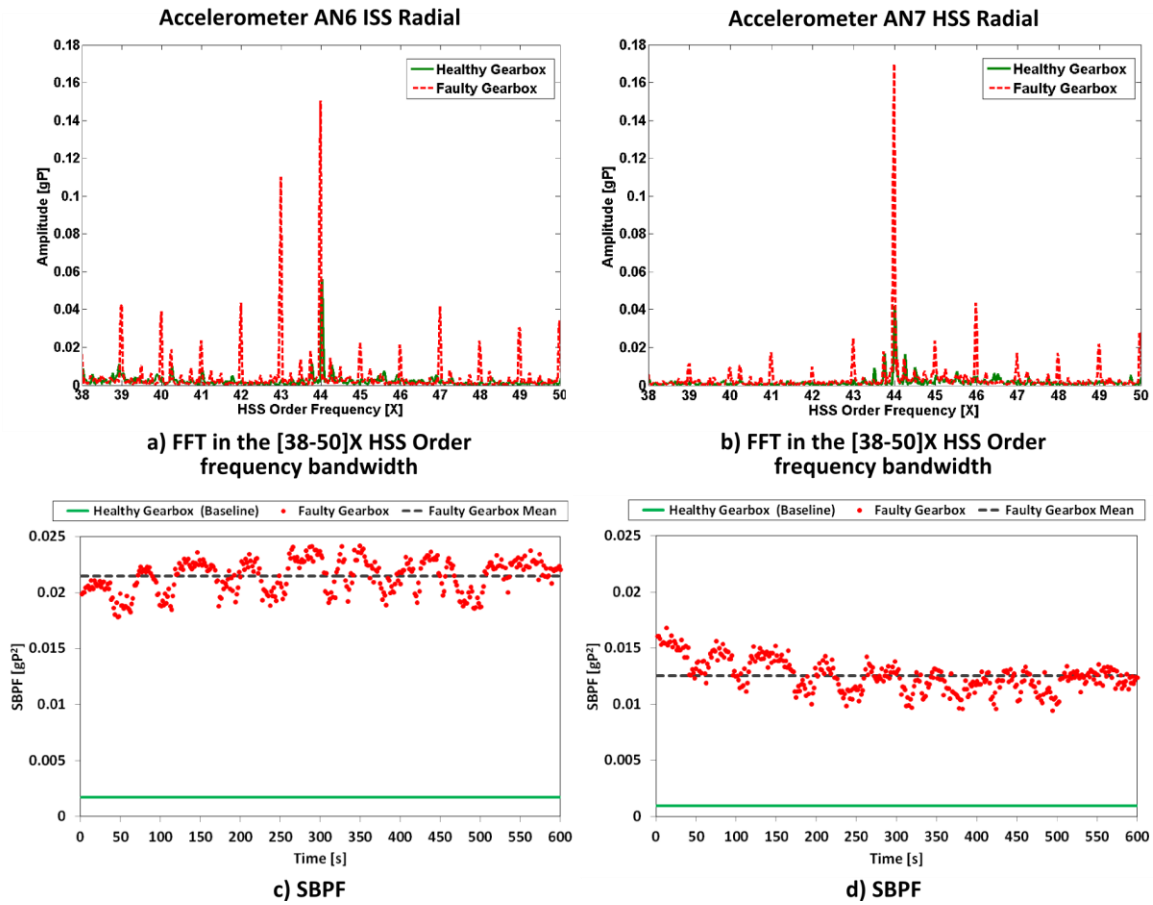

Figure 8: **Vibration FFT spectra and SBPF plots for 2 accelerometer positions on healthy (green) and faulty (red) identical 750 kW gearboxes.**

4.3. Algorithm Implementation

To quantify these observations from the vibration data, SBPF values were extracted from the baseline spectrum and the 375 degraded gearbox spectra. The results are shown in Figure 8 c) and d) for AN6 and AN7, respectively. In both cases, the SBPF magnitude is much larger for the degraded gearbox compared to the baseline gearbox, representing an average value of 0.021 $(gP)^2$ and 0.013 $(gP)^2$, respectively. From the SBPF methodology, there is a strong indication that there is damage on the high-speed shaft pinion. These results, on a full-size 750 kW gearbox, provide further credibility to the SBPF algorithm, already proven on the 30 kW WTCMTR, for timely detection and diagnosis of gear damage.

In this case, the use of vibration signals collected from two independent accelerometers located in strategic positions on the gearbox casing improves the confidence in the SBPF fault detection and diagnosis capability, eventually reducing false alarms. This is particularly interesting when considering than one issue around CMS data interpretation is to rely on a single signal, which could lead to false alarms from the monitoring process [10].

5. Discussion

Experimental work on the low-power Durham WTCMTR has allowed the implementation of repeated seeded-fault conditions under controlled conditions. The developed SBPF algorithm allows the assessment of gear fault severity by tracking progressive tooth gear damage during variable speed and load operating conditions of the test rig. The performance of the proposed technique has then been successfully tested on signals from a field test of a full-size WT gearbox that has sustained gear damage.

The SBPF detection sensitivity to tooth damage has been calculated by determining, for each load condition, the percentage change of the SBPF value. For each case, the SBPF detection sensitivity (%SBPF) between faulty and healthy conditions has been defined as

$$\%SBPF = \frac{SBPF_f - SBPF_h}{SBPF_h} * 100 \qquad (6)$$

where $SBPF_h$ and $SBPF_f$ are the SBPF values for the healthy and faulty cases, respectively. Table 2 summarises the average SBPF detection sensitivities to HSS pinion damage for the 30 kW Durham gearbox and the 750 kW NREL gearbox data-sets.

Table 2: Durham (30 kW) and NREL (750 kW) gearbox average SBPF detection sensitivity.

Gearbox	HSS Pinion Fault Severity	Accelerometer Location	Average %SBPF
Durham - 30 kW seeded-fault tests	Early Stages of Tooth Wear	HSS Vertical	100%
	Missing Tooth	HSS Vertical	320%
NREL - 750 kW gearbox datasets	Severe Scuffing	AN6 ISS Radial	1140%
	Severe Scuffing	AN7 HSS Radial	1251%

In the case of the Durham 30 kW gearbox data-set, the sensitivity analysis shows that the SBPF technique proves successful in the detection of both early and final stages of gear tooth damage, with average detection sensitivities of 100% and 320%, respectively. It is evident the influence of the fault severity on the SBPF detection sensitivity values; the more damaged is the pinion the easier is to discriminate the fault.

In the case of the NREL data-set, although the gearbox damage was more complex than in a typical operational WT [19] and the data-set provided refers to only one speed and load operational condition, the SBPF detection and diagnostics technique proves successful in the detection of HSS pinion damage, with an average detection sensitivity of 1140% and 1251% for the AN6 ISS radial and AN7 HSS radial accelerometers, respectively. Because the analysed data-set contains multiple gearbox progressed faults, it is believed that in the SBPF diagnostic performance could be improved when deployed in the field, bearing in mind the smaller number of faults usually presented during the early stages of gearbox fault evolution.

The proposed SBPF algorithm facilitates the monitoring analysis, reducing each FFT spectrum to only one parameter for each data acquisition. By automating the condition monitoring of the gears, SBPF reduces the quantity of vibration information that WT operators must handle, providing improved detection and timely decision-making capabilities. SBPF can be monitored over time, trended, and

compared to one or more predetermined threshold levels to provide warnings and alarms to operators.

The knowledge of the gearbox load is fundamental to apply effectively the SBPF technique. The current commercial available CMSs usually provide information on the turbine load. This will allow the SBPF technique to work in context with the gearbox load. Otherwise, in case the turbine load is not available, the Operator has to take SBPF measurements only when the machine is at its full load.

The SBPF methodology, based on the analysis of the dynamics of the gears, can easily be scaled to higher WT power levels. However, this would probably imply an increase in the spectral background noise because of the higher complexity of WT drive trains compared to the small-scale WTCMTR.

For gearbox parallel stages, SBPF is easily applicable to the harmonics of each fundamental gear mesh frequency using both gear and pinion SBs, once the multi-stage gearbox configuration and the number of teeth of each gear element are known. This information allows for the calculation of the gear damage features, such as the meshing frequencies, their second harmonic and the spacing of the SBs due to gear wear modulation phenomena for each stage, and the extraction of the corresponding SBPF values. For planetary stages, the analysis of the SB patterns could be more complicated because of the low mechanical transmissibility from gear components and the multiple contact points between each planet gear meshing and the sun and ring gear.

6. Conclusions

This paper has proposed an experimental side-band algorithm for automatic WT gear tooth fault detection and diagnosis, which has been validated by analysing vibration signals from a full-size WT gearbox with HSS pinion faults. The following specific conclusions arise:

- The SBPF algorithm proved effective in detecting the presence of gear damage introduced into a 30 kW Test Rig gearbox, i.e., damage location, and in identifying the precise damaged gear, i.e., damage diagnosis, with a detection sensitivity of 100% to 320%.

- The SBPF successfully allowed the assessment of gear fault severity on the Test Rig by tracking progressive tooth damage, from the early stages of development, during variable speed and load conditions.
- The experimentally defined SBPF technique has also been successfully tested against vibration data from an NREL 750 kW WT gearbox, which had experienced severe high-speed shaft gear set scuffing, with a detection sensitivity of 1140% and 1251%.
- Confidence in the NREL gearbox results is enhanced by the strong SBPF detection and diagnosis evidence from two independent accelerometers.
- The proposed methodology is relatively simple to implement into a commercial WT CMS for automatic gear fault detection and diagnosis.
- The generation of SBPF trends from the vibration spectra and the definition of magnitude thresholds for the fault severity levels could indicate to a WT operator when a maintenance action needs to be performed.
- SBPF can be easily adapted to detect gear damage on all the WT gearbox parallel stages, while its applicability to planetary stages still requires more investigation.
- Compared to the conventional FFT approach used in current commercial vibration-based CMSs, requiring time-consuming visual spectra analysis, the SBPF approach enables automatic detection and diagnosis of gear faults with low risk of false alarms. This will lead to increased accuracy of WT drive-train vibration-based condition monitoring.

7. Acknowledgments

This work was funded as part of the UK EPSRC Supergen Wind Energy Technologies programme, EP/H018662/1. The authors thank NREL for its support for this work and for providing the vibration data used for the validation of the SBPF algorithm.

8. References

1. EWEA, 'Wind Energy, Statistics & Targets'. European Wind Energy Association Report, 2013, available at http://www.ewea.org/fileadmin/files/library/publications/statistics/Factsheets.pdf, last accessed 23rd April 2013

2. McMillan, D., and Ault, G.W.: 'Quantification of Condition Monitoring Benefit for Offshore Wind Turbines', Wind Engineering, 2007, 31, (4), pp. 267-285
3. Walford, C.A., 'Wind Turbine Reliability: Understanding and Minimizing Wind Turbine Operation and Maintenance Costs'. Sandia National Laboratories Report SAND2006-1100, March 2006, available at http://prod.sandia.gov/techlib/access-control.cgi/2006/061100.pdf, last accessed 20th April 2013
4. Wiggelinkhuizen, E., Verbruggen, T., Braam, H., Rademakers, L., Xiang, J.P., and Watson, S.: 'Assessment of Condition Monitoring Techniques for Offshore Wind Farms', Journal of Solar Energy Engineering-Transactions of the Asme, 2008, 130, (3), p. 9
5. Hyers, R.W., McGowan, J.G., Sullivan, K.L., Manwell, J.F., and Syrett, B.C.: 'Condition Monitoring and Prognosis of Utility Scale Wind Turbines', Energy Materials: Materials Science and Engineering for Energy Systems, 2006, 1, (3), pp. 187-203
6. Faulstich, S., Hahn, B., and Tavner, P.J.: 'Wind Turbine Downtime and Its Importance for Offshore Deployment', Wind Energy, 2011, 14, (3), pp. 327-337
7. Sheng, S.: 'Investigation of Various Condition Monitoring Techniques Based on a Damaged Wind Turbine Gearbox'. Proceedings of the 8th International workshop on Structural Health Monitoring, Condition-based Maintenance and Intelligent Structures, Stanford, California, September 13-15, 2011
8. Hameed, Z., Hong, Y.S., Cho, Y.M., Ahn, S.H., and Song, C.K.: 'Condition Monitoring and Fault Detection of Wind Turbines and Related Algorithms: A Review', Renewable and Sustainable Energy Reviews, 2009, 13, (1), pp. 1-39
9. Wilkinson, M.R., Spinato, F., and Tavner, P.J.: 'Condition Monitoring of Generators and Other Subassemblies in Wind Turbine Drive Trains'. IEEE International Symposium on Diagnostics for Electric Machines, Power Electronics and Drives, SDEMPED 2007, Sept. 6-8, 2007
10. Feng, Y., Qiu, Y., Crabtree, C.J., Long, H., and Tavner, P.J.: 'Monitoring Wind Turbine Gearboxes', Wind Energy, Article first published online: 16 JUL 2012, DOI: 10.1002/we.1521
11. Walford, C., and Roberts, D., 'Condition Monitoring of Wind Turbines: Technology Overview, Seeded-Fault Testing and Cost-Benefit Analysis'. EPRI Report No. 1010419, 2006
12. Gray, C.S., and Watson, S.J.: 'Physics of Failure Approach to Wind Turbine Condition Based Maintenance', Wind Energy, 2010, 13, (5), pp. 395-405
13. Crabtree, C.J.: 'Operational and Reliability Analysis of Offshore Wind Farms'. Proceedings of the Scientific Track of the European Wind Energy Association Conference, Copenhagen, Denmark, April 16-19, 2012
14. Tavner, P.J.: 'Offshore Wind Turbines: Reliability, Availability and Maintenance' (The Institution of Engineering and Technology, 2012, 1st edn)
15. Crabtree, C.J., and Zappalà, D., 'Survey of Commercially Available Condition Monitoring Systems for Wind Turbines'. Supergen Wind Energy Technologies Consortium Report, 2012, available at www.supergen-wind.org.uk, last accessed 2nd September 2012
16. Randall, R.B.: 'Vibration-Based Condition Monitoring: Industrial, Aerospace and Automotive Applications' (John Wiley & Sons, Ltd, 2011)
17. García Márquez, F.P., Tobias, A.M., Pinar Pérez, J.M., and Papaelias, M.: 'Condition Monitoring of Wind Turbines: Techniques and Methods', Renewable Energy, 2012, 46, (0), pp. 169-178

18. Yang, W., Tavner, P.J., Crabtree, C.J., Feng, Y., and Qiu, Y.: 'Wind Turbine Condition Monitoring: Technical and Commercial Challenges', Wind Energy, Article first published online: 1 AUG 2012, DOI: 10.1002/we.1508
19. Sheng, S.: 'Wind Turbine Gearbox Condition Monitoring Round Robin Study - Vibration Analysis'. NREL Report No. TP-5000-54530, 2012, available at http://www.nrel.gov/publications/, last accessed 26th November 2012
20. Crabtree, C.J.: 'Condition Monitoring Techniques for Wind Turbines'. PhD Thesis, Durham University, UK, 2011
21. Randall, R.B.: 'A New Method of Modelling Gear Faults', Journal of Mechanical Design-Transactions of the ASME, 1982, 104, (2), pp. 259-267
22. Goldman, S.: 'Vibration Spectrum Analysis: A Practical Approach' (Industrial Press Inc., 1999, 2nd edn)
23. Mobley, R. K.: 'Vibration Fundamentals' (Newnes/Butterworth-Heinemann, 1999, 1st edn)
24. Zappalà, D., Tavner, P.J., and Crabtree, C.J.: 'Gear Fault Detection Automation Using Windcon Frequency Tracking'. Proceedings of the Scientific Track of the European Wind Energy Association Conference, Copenhagen, Denmark, April 16-19, 2012
25. Musial, W., and McNiff, B.: 'Wind Turbine Testing in the NREL Dynamometer Test Bed'. Proceedings American Wind Energy Association's WindPower 2000 Conference, Palm Springs, CA, April 30-May 4, 2000
26. Errichello, R., and Muller, J., 'Gearbox Reliability Collaborative Gearbox 1 Failure Analysis Report'. NREL Report NREL/SR-5000-530262, 2012, available at http://www.nrel.gov/docs/fy12osti/53062.pdf, last accessed 15th September 2012